Synthesis of Novel (bis-)1,5-Disubstituted-1*H*-tetrazole-Decorated Monomers and Their Respective Polymers via Thiol-ene Polymerization

Meryem S. Akdemir, Marina Simian, Patrick Theato,* and Hatice Mutlu*

Over the years, nitrogen-rich functional groups like tetrazole and its derivatives have received increasing interest in the chemistry of small molecules. There is a continuously growing interest in polymers decorated with nitrogen for potential biomedical applications because of their broad range of biological properties, such as being antibacterial, anticarcinogenic, and anti-inflammatory. On this premise, a new synthesis route is reported for nitrogen-decorated polymers via the combination of Ugi-azide four-multicomponent reaction (UA-4MCR) and thiol-ene polymerization. Accordingly, α,ω-diene monomers decorated with (bis-)1,5-disubstituted-1*H*-tetrazoles (bis-1,5-DS-Ts) are synthesized by using the UA-4MCR. Subsequently, the light-induced thiol-ene polymerization facilitates the efficient synthesis of novel tetrazole-decorated polymers with apparent number average molecular mass (M_n) up to 62 000 g mol^{-1}, which are characterized for their chemical, thermal, and optical properties. The comprehensive characterization of the synthesized polymers is paving the way toward a wealth of opportunities, ranging from biomaterials to energy storage—relevant materials.

1. Introduction

The chemistry focusing on five-membered aromatic nitrogen heterocycles is currently receiving a significant research interest in organic chemistry for developing novel molecules.[1] Indeed, five-membered aromatic nitrogen heterocycles are widely used in the development of synthetic strategies to obtain complex and structurally diverse libraries of bioactive compounds.[2] On the one hand, among the broad spectrum of heterocyclic substances, aliphatic and aromatic substituted tetrazoles, particularly nitrogenous heterocyclic 1,5-disubstituted-1*H*-tetrazoles (**1,5-DS-Ts)**, are gaining ever-increasing importance due to their remarkable biological activities (e.g., antiviral, anti-inflammatory, antibacterial, and antifungal).[3–5] In fact, 1,5-disubstituted-1*H*-tetrazoles derivatives have demonstrated to be appropriate bioisosteres of the *cis*-amide bond of peptides due to the ability to adjust their confirmation (**Scheme 1**A).[6,7] Unfortunately, **1,5-DS-Ts** do not occur naturally.[3] On the other hand, synthetic polymers decorated with aliphatic substituted 1,5-tetrazole units (either in the main chain or as pendant groups) appear to be less investigated compared to their small molecule counterparts,[8–11] mainly due to synthetic challenges taking place either during the synthesis of the respective monomer or the respective polymerizations.[8,12,13] In fact, an in-depth literature survey revealed that most of the existing examples of aliphatic substituted tetrazole-decorated polymers are based on carbon-carbon backbone with tetrazole side chains.[13–16] Those polymers are synthesized either via the polyaddition reactions of tetrazole-decorated dihydrazine monomers with diisocyanate or the radical polymerization of

M. S. Akdemir, P. Theato, H. Mutlu
Soft Matter Synthesis Laboratory
Karlsruhe Institute of Technology (KIT)
Hermann-von-Helmholtz-Platz 1
D-76344 Eggenstein-Leopoldshafen, Germany
E-mail: patrick.theato@kit.edu; hatice.mutlu@uha.fr

H. Mutlu
Institut de Science des Matériaux de Mulhouse
UMR 7361 CNRS/Université de Haute Alsace
15 rue Jean Starcky, Mulhouse Cedex 68057, France

P. Theato
Institute for Chemical Technology and Polymer Chemistry (ITCP)
Karlsruhe Institute of Technology (KIT)
Engesserstr.18, D-76131 Karlsruhe, Germany

P. Theato
Institute for Biological Interfaces 3 (IBG 3)
Karlsruhe Institute of Technology (KIT)
Hermann-von-Helmholtz-Platz 1, D-76344 Eggenstein-Leopoldshafen, Germany

M. Simian
Instituto de Nanosistemas
Universidad Nacional de San Martín (INS-UNSAM)
Av. 25 de Mayo 1021, San Martín, Buenos Aires B1650KNA, Argentina

**ADVANCED
SCIENCE NEWS**

www.advancedsciencenews.com

**Macro-
molecular
Chemistry** and **Physics**

www.mcp-journal.de
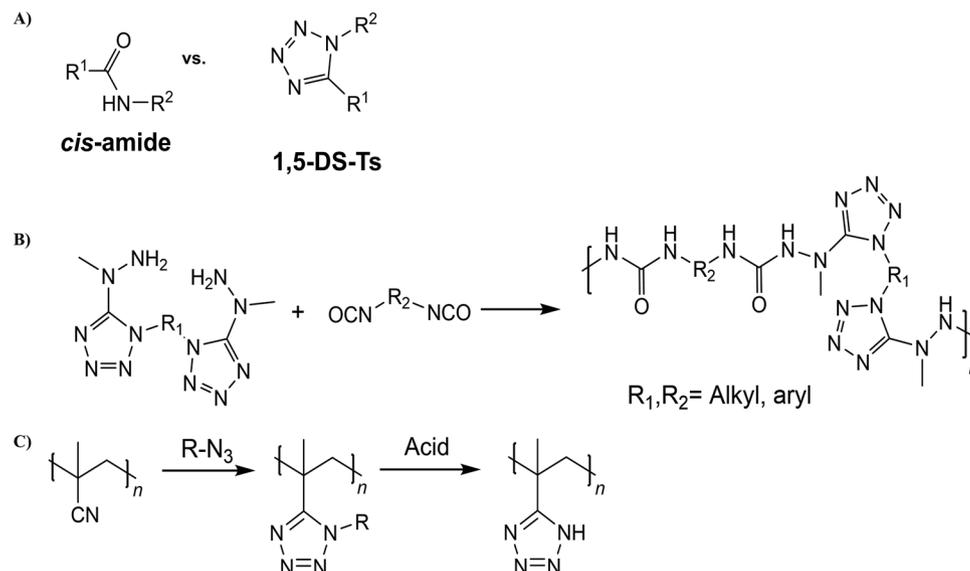
Scheme 1. A) General structures of the *cis*- amide bond of the peptides (left) and bis-**1,5-DS-T** structure of the tetrazole moiety (right) as a mimic of a *cis*-peptide bond; B,C) Previously reported methods for the synthesis of **1,5-DS-T** containing polymers.[17,19,20]

1-(vinyl-1*H*-tetrazole) as shown in Scheme 1B.[17,18] Alternatively, the functional group conversion reaction of polyvinylnitrile into the tetrazole moiety via a [2+3] cycloaddition reaction with azide derivatives acid has been reported (Scheme 1C).[19–21]

Hence, due to the broad plethora of potential applications of aliphatic substituted tetrazole-containing polymers in the field of biomedical and energy-relevant materials research, there is an ever-increasing demand for the development of straightforward and efficient polymerization. On the one hand, multi-component reactions (MCRs, such as Passerini,[22] Biginelli,[23] or Ugi[24]) and their relevant polymerization approaches have appeared as suitable methods, as those reactions enable the generation of a single product from three or more starting materials in a one-pot manner. Indeed, MCRs and multi-component polymerizations (MCPs) are generally considered as sustainable synthesis tools as they provide operational simplicity under mild conditions with high efficiency and deliver a great diversity of product structures. Particularly, the Ugi four-component reaction (U-4CR), which was discovered in 1982 by Ivar Karl Ugi,[25] is one of the most significant and well-known MCRs.[3] A slightly modified version, i.e., the Ugi-azide four-multicomponent reaction (UA-4MCR), a variant in which an azide (i.e., azidotrimethylsilane (TMSN$_3$)) is utilized instead of carboxylic acid, has been used as a key step to obtain various systems containing the 1,5-disubstituted-tetrazole scaffold.[26] It is important to note that the UA-4MCR has neither been utilized for α,ω-diene monomer syntheses nor for polymerization methods, although it provides diversity as well as complexity and allows the preparation of highly attractive **bis-1,5-DS-T** derivatives in one-pot manner from commercially available starting materials.[27]
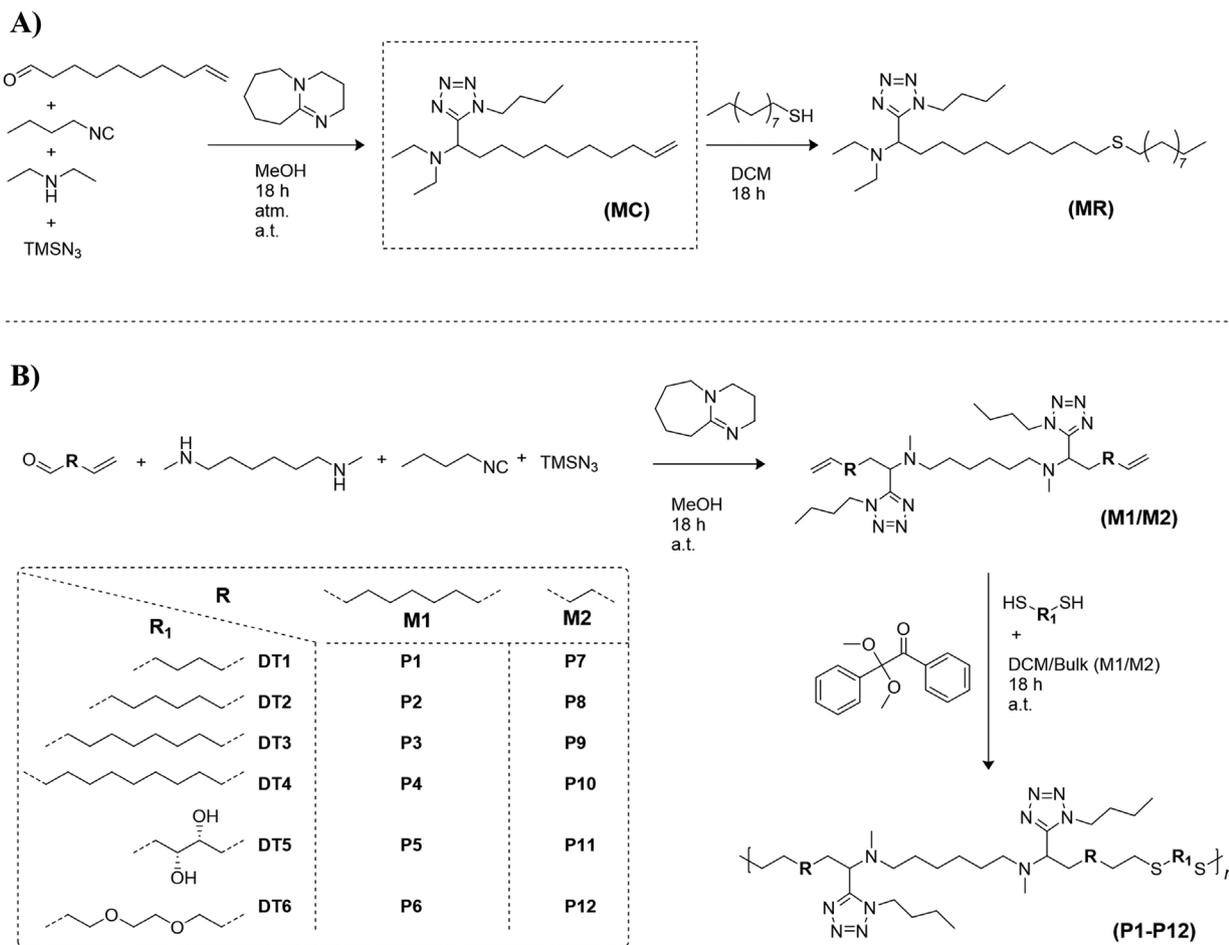
On the other hand, the thiol-ene reaction, the so-called "click"-reaction between a thiol compound (–SH) and an olefin bond, is one of the well-established techniques in the field of polymer chemistry. The thiol-ene click reaction can take place with base-catalyzed electron-deficient alkenes or by a radically initiated reaction with non-activated olefins, thus has been utilized not only

to deliver diverse macromolecular structures ranging from linear polymers to networks, but also for post-polymerization and surface modifications.[28,29] Notably, in contrast to thermally initiated thiol-ene systems, photochemical approaches allow selective reactions to occur efficiently at ambient temperatures. Still, the implementation of the light-induced thiol-ene reaction as a polymerization approach to deliver tetrazole-decorated polymers is not fully explored. Accordingly, this work aims to develop **1,5-DS-T** containing polymers by utilizing the photo-induced (i.e., 365 nm) thiol-ene polyaddition reaction. For this purpose, a **1,5-DS-T** tethered model compound via UA-4MCR has been synthesized to get the necessary insights and a general understanding of the behavior of tetrazole formation, and the feasibility of thiol-ene reaction on such compounds (**Scheme 2**A). Subsequently, an efficient synthetic route for a novel type of **bis-1,5-DS-T** α,ω-diene monomers has been developed. Consequently, those monomers (Scheme 2B) were further polymerized with a series of different thiol derivatives to broaden the toolbox of bis-1,5-disubstituted-1*H*-tetrazole-decorated polymers. Last but not least, all obtained polymers were analyzed in detail using size exclusion chromatography (SEC), nuclear magnetic resonance (NMR), attenuated total reflection infrared spectroscopy (ATR-IR), thermal gravimetric analysis (TGA) and differential scanning calorimetry (DSC), along UV-vis and fluorescence spectroscopy.

2. Results and Discussion

2.1. Synthesis and Characterization of the 1,5-DS-T Model Compound and Its Respective Model Thiol-ene Reaction

Recently, Levkin and colleagues have demonstrated the UV-induced nitrile imine mediated tetrazole-thiol reaction on 2,5-diphenyltetrazole derivatives.[30] Therefore, it was essential to ensure that 1,5-disubstituted tetrazole derivatives remain intact during the light-induced reaction with the thiol derivatives. Accordingly, a **1,5-DS-T** containing model compound (**MC**)

**ADVANCED
SCIENCE NEWS**

www.advancedsciencenews.com

|M| macro-
molecular
Chemistry and Physics

www.mcp-journal.de

A)

B)

Scheme 2. Schematic representation of: A) the Ugi-azide four-multicomponent reaction (UA-4MCR) to provide **1,5-DS-T** containing model compound (**MC**) and its light-induced ($\lambda = 365$ nm) model thiol-ene reaction (**MR**). B) Synthesis approaches for the preparation of **1,5-DS-T** containing α,ω-diene monomers **M1** and **M2** to deliver **1,5-DS-T** containing polymers via thiol-ene reaction with dithiols (e.g., 1,4-butanedithiol (**DT1**), 1,6-hexanedithiol (**DT2**), 1,8-octanedithiol (**DT3**), 1,9-nonanedithiol (**DT4**), dithiothreitol (**DT5**) and 3,6-dioxa-1,8-octanedithiol (**DT6**) which are represented in table from **P1-P12** under light initiation ($\lambda = 365$ nm). R and R1 donate different functional groups as they are depicted within the table.

was synthesized by reacting 10- undecenal, butyl isocyanide diethylamine, and TMSN$_3$ in the presence of the catalyst 1,8-diazabicyclo(5.4.0)undec-7-ene (DBU) in methanol under inert atmosphere at ambient temperature by adopting a recently reported procedure (Scheme 2A).[27,31] The chemical structure of the **MC** was confirmed via 1D and 2D NMR spectroscopy (**Figure 1A** (shown in red) and Figure S1, Supporting Information). Crucially, the presence of magnetic resonance of the only proton associated with the tetrazole moiety was detected at ≈ 3.8 ppm. Furthermore, it was a prerequisite that the olefin end groups of the targeted model compound also remain intact during the synthesis, which could be affirmed by the presence of the magnetic resonances arising from the alkene functional group, observed at ≈ 5.7 and ≈ 5.0-4.8 ppm in Figure 1A. Moreover, the magnetic resonances detected at 115 and 139 ppm in ^{13}C-NMR could be attributed to the olefin functionality (Figure S2, Supporting Information). In addition, we observed the magnetic resonance at 155 ppm, which corresponds to the only carbon atom in the 1,5 disubstituted tetrazole moiety. Additionally, the absorption bands at 1056 and 1382 cm^{-1} in the ATR-IR spectrum could be assigned to the antisymmetric stretching mode of N–N and vibration band

of N=N bonds, respectively (red line, Figure 1B). Particularly, the bands detected at 1234 and 1114 cm^{-1}, due to the C=N and C–N stretching, confirmed the presence of **1,5-DS-T** unit in the respective compound (red line, Figure 1B). Accordingly, an initial investigation of a light-initiated ($\lambda = 365$ nm) thiol-ene reaction, whose product is depicted as **MR**, has been performed by using 1-dodecanthiol (1:1 thiol-to-ene molar ratio) and **MC** in the presence of 2,2-dimethoxy-2-phenylacetophenone (DMAP) as the photoinitiator. The resulting product, i.e., **MR**, was obtained with a reasonable total yield of 98% upon purification by column chromatography, and the chemical structure was confirmed via ^{1}H NMR analysis. In fact, the detailed NMR analysis of the isolated product, which is shown in Figure 1A, clearly verified that no photolytic decomposition of **1,5-DS-T** took place during the light-induced thiol-ene reaction. Explicitly, it was observed that magnetic resonance c at ≈ 3.8 ppm, associated with tetrazole moiety, remained intact. Indeed, an evaluation of the comparative NMR and SEC data of the **MC** with the crude reaction mixture of **MR** prior to the purification (Figure S3, Supporting Information) validated not only the efficiency of the thiol-ene reaction, but also that no degradation took place. Aside, the comparative
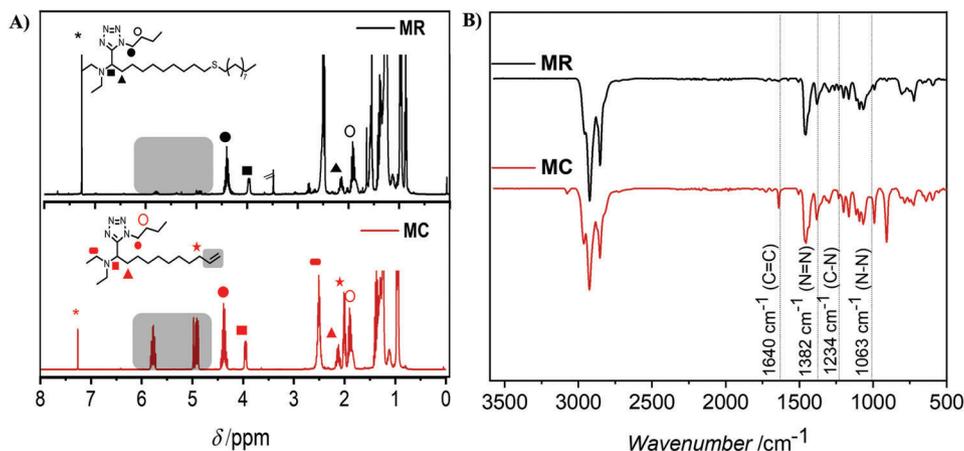
ADVANCED
SCIENCE NEWS

www.advancedsciencenews.com

{M} macro-
molecular
Chemistry and Physics
www.mcp-journal.de

Figure 1. Comparative: A) ^{1}H-NMR (400 MHz, CDCl$_3$) and B) ATR-IR spectra of **MC** (red line) and **MR** (black line), respectively.

ATR-IR spectra of the isolated **MC** (red line, Figure 1B) and **MR** (black line, Figure 1B) verified that the structure of the **1,5-DS-T** remained stable.

2.2. Synthesis and Characterization of 1,5-DS-T Decorated α,ω-Diene Monomers M1 and M2

Upon confirming that the 1,5-disubstituted tetrazole unit is unreactive during the photo-induced thiol-ene reaction, in the next step, **bis-1,5-DS-T** α,ω-diene monomers were synthesized by adopting the above-mentioned procedure (Section A.2.2 in the Supporting Information). To ensure the feasibility of the synthetic strategy, it was fundamental to have two terminal olefin handles in the monomer structure to allow for a polyaddition with dithiol derivatives. Thus, targeted α,ω-diene monomers **M1** and **M2** (shown in Scheme 2B) were synthesized by using 2 eq. of the appropriate aldehyde[32] (i.e.,10-undecenal and 4-pentenal for **M1** and **M2**, respectively), 1 eq. of the diamine N,N-dimethyl-1,6-hexanediamine,[33] 2 eq. of butyl isocyanide, 2 eq. of azidotrimethylsilane (TMSN$_3$) and DBU (as a catalyst) in MeOH (1 M) at ambient temperature for 18 h (Scheme 2B). Subsequently, the targeted monomers were isolated in reasonably good yields (95% and 89% for **M1** and **M2**, respectively) upon column chromatography (DCM:MeOH (19:1)). The chemical structure of α,ω-diene monomers (**M1** and **M2**) was confirmed by 1D and 2D-NMR (compare Figures S4 and S5, Supporting Information) in addition to ATR-IR spectroscopy (Figure S6, Supporting Information). On the one hand, the magnetic resonances at ≈5.7 and 3.8 ppm in ^{1}H NMR spectrum corresponding to the protons on the terminal olefin and **bis-1, 5-DS-T** moieties, respectively, for both **M1** and **M2**, were observed. On the other side, as in the case of the ATR-IR analysis for **MC**, all analogous bands confirming the presence of tetrazole moiety can be detected in the comparative spectra for **M1** and **M2** (Figure S6, Supporting Information).

2.3. Synthesis of 1,5-DS-T Decorated Polymers via Light-Induced Thiol-ene Polyaddition

Motivated by the successful results of the test reaction performed with **MC**, the light-induced thiol-ene polymerizations of **M1** and

M2 were conducted in the presence of stoichiometric amount of various dithiol derivatives. It is important to mention that a one-pot tandem multicomponent polymerization approach in which the respective dithiol derivative is reacted with the precursors delivering the tetrazole-decorated monomers (e.g., aldehyde derivative, diamine N,N-dimethyl-1,6-hexanediamine, butyl isocyanide, TMSN$_3$, and DBU) is not feasible. Indeed, an in-depth literature survey reveals that thiol derivatives (aliphatic and aromatic) are reacting efficiently with isocyanides both in radical,[34,35] and nucleophilic[36] manner, which in turn will hinder any polymer formation with the targeted chemical structure (i.e., (bis-)1,5-disubstituted-1H-tetrazole). Nevertheless, to overcome the disadvantages of low monomer mobility and reactivity resulting in a decreased degree of polymerization (DP) and number average molecular mass (M_n), 1,9-nonanedithiol (**DT4**) has been initially employed in the polymerization. Indeed, **DT4**, as the longest alkyl chain dithiol derivative, has the lowest density (i.e., 0.95 g mL^{-1})[37] and the most flexible aliphatic chain length compared to all dithiol derivatives that have been used to show the modularity of the approach. In fact, it has already been reported that step-growth polymerizations[38] performed with longer alkyl chain monomers result in polymers that may be more easily diffuse even in solid-state polymerization under the same temperature/time conditions compared to the shorter alkyl chain derivatives. Moreover, shorter-chain monomers usually depict a greater degree of intramolecular cyclization during step-growth polymerization.[39] Accordingly, **M1** was reacted efficiently with **DT4** in 1.0 M dichloromethane (DCM) at ambient temperature (a.t.) overnight (ON) in the presence of 0.3 wt.% DMPA to yield polymer **P4**, which was isolated with an apparent number average molecular mass (M_n) of 40 200 g mol^{-1} (with dispersity, Đ, of 2.0 as determined by size exclusion chromatography (SEC) relative to polymethylmethacrylate (PMMA) standards in tetrahydrofuran (THF) as eluent). Complementary to SEC, ^{1}H-NMR spectroscopy of **P4** unambiguously confirmed the formation of the targeted poly(thioether) decorated with two 1,5-tetrazole units in each repeating unit and revealed a very high monomer conversion as judged from the decreased signal intensity of olefinic protons at 5.7 and 4.9 ppm (Figure S7, Supporting Information). In the similar manner, the presence of the magnetic resonances at 2.5 and 1.9 ppm corresponding to the

Table 1. Molecular characterization and thermal analysis of tetrazole-decorated polymers (**P1–P12**) obtained via thiol-ene polyaddition reaction. Typical reaction conditions were as follows: monomer (1eq.), dithiol derivative (2 eq.), and light-initiator (DMPA, 0.3 wt.%) were reacted at $\lambda = 365$ under inert conditions.

Polymer	Dithiol[a]	M_n [g mol^{-1}] SEC[b]	$Đ [M_w/M_n]$ SEC	$T_{d, 5\%}$ [°C] TGA[c]	T_g [°C] DSC[d]
P1[*]	DT1	34 200	5.0	299	−31
P2[*]	DT2	23 800	1.6	298	−37
P3[*]	DT3	62 800	3.2	301	−32
P4[*]	DT4	40 200	2.3	301	−34
P5[*]	DT5	49 100	2.9	288	−13
P6[*]	DT6	42 500	2.5	301	−42
P7[**]	DT1	24 800	1.3	280	−20
P8[**]	DT2	35 600	1.4	280	−29
P9[**]	DT3	38 500	1.4	286	−23
P10[**]	DT4	50 100	1.9	286	−28
P11[**]	DT5	20 500	1.9	267	−21
P12[**]	DT6	37 300	1.4	292	−32

[*]M1 has been used as the monomer; [**]M2 has been used as monomer; [a] Dithiol derivatives:1,4-butanedithiol (**DT1**), 1,6-hexanedithiol (**DT2**), 1,8-octanedithiol (**DT3**), 1,9-nonanedithiol (**DT4**), dithiothreitol (**DT5**) and 3,6-dioxa-1,8-octanedithiol (**DT6**); [b] Determined by SEC using THF as an eluent; [c] The decomposition temperature ($T_{d, 5\%}$) defined as the temperature at 5% weight loss was detected by TGA; [d] The glass transition temperature (T_g) observed during the second heating measurement via DSC analysis.

protons at the α- and β-positions adjacent the thioether bond, in addition to the tetrazole proton appearing at 3.8 ppm, confirmed the expected chemical structure of the repeating units of the polymer. Moreover, ATR-IR analysis of polymer **P4** (Figure S8, Supporting Information) indicated that the C=C absorption bands (3104 and 1640 cm^{-1}), which correspond to alkene functionalized handles of **M1**, have disappeared, while the characteristic absorption bands of tetrazole unit detected at 1056, 1114, 1234, and 1382 cm^{-1} remained intact. Upon the successful polymerization of **M1**, the same conditions have been adopted to polymerize **M2**. Nevertheless, **M2** failed to polymerize under the mentioned conditions (i.e., 1.0 M DCM, ON, a.t.). As it has been already mentioned, Kricheldorf explored cyclic oligomerization competing with the polymerization in step-growth processes for short alkyl chain length derivatives[35] and described self-dilution as a common characteristic for conventional step-growth polymerization of such monomers. Therefore, we assume that possible cyclic oligomerization could take place between the reactive groups of the short-chain α,ω-diene monomer **M2** and prevented the polymer formation. Thus, a bulk polymerization of **M2** with **DT4** has been performed alternatively under $\lambda = 365$ nm for 24 h, which resulted in polymer formation, i.e., **P10** ($M_n = 50 100$ g mol^{-1}, $Đ = 1.5$). The chemical structure of **P10** was also confirmed in an analogous manner to **P4** by NMR and IR spectroscopy (Figures S9–S10, Supporting Information). Subsequently, the photo-initiated thiol-ene polymerization was employed to produce a family of polymers of the new tetrazole-decorated α,ω-diene monomers **M1** and **M2** in the presence of various dithiols (**DT1-DT6**) depicted in Scheme 2B. Accordingly, some exemplary NMR and IR results of the obtained polymers are presented in Figures S11 and S12, Supporting Information. It is important to note that the polymerization of **M1** was performed in DCM, whereas **M2** was usually polymerized in bulk. In general, polymers of moderate number average molecular mass

(20 500 < M_n < 62 800 g mol^{-1}) and expected step-growth dispersity values (1.4 < $Đ$ < 3.2) were obtained for the aliphatic dithiol derivatives as shown in **Table 1**. Surprisingly, the polymerization of **M1** with **DT1** delivered a polymer with a considerably high dispersity value ($Đ$ of 5.0, compare Table 1, Entry 1, and **Figure 2**A). In fact, high dispersity values are rather typical for polymer chains having a relatively high tendency of cyclization.[40] The latter is particularly taking place during the step-growth polymerization of any short alkyl chain length derivatives, such as **DT1**. In point of fact, Kricheldorf,[41] in many of his works, has emphasized that decreasing the alkene length in any reactive bifunctional monomer is inducing the cyclization tendency of the system (defined as the ratio of rate constants of cyclization vs. chain extension). Therefore, a typical step-growth polymer can contain predominantly linear species and a varying amount of cyclic species.[42] Actually, bimodal molecular weight distributions are usually detected in such polymerizations as the cyclic products are mainly oligomers, whereas the linear chains have high molecular weight.[43] On the contrary, lower $Đ$ values were obtained for samples prepared in bulk [as for **P7** ($Đ$ of 1.3), which was synthesized from **M2** and **DT1**, both monomers possessing the shortest methylene spacers] and with only moderate conversion. Actually, the decrease of the dispersity by applying bulk conditions is predictable as the Ruggli—Ziegler–Dilution Principle, which in turn states that the lower concentration of reagents leads to a higher amount of cyclic molecules and a lower degree of polymerization.[44] Delightfully, polar dithiol monomers such as dithiothreitol (**DT5**) and 3,6-dioxa-1,8-octanedithiol (**DT6**) also resulted in polymers (Entries 5, 6, 11, and 12 in Table 1). Indeed, we observed that the pendant polar hydroxyl in addition to the polar 1,5-disubstituted tetrazole groups allow polymers (**P5** and **P11**) to be good soluble not only in conventional organic solvents, such as THF, DCM, and N,N-dimethylformamide (DMF), but also in a polar solvent, such as methanol.
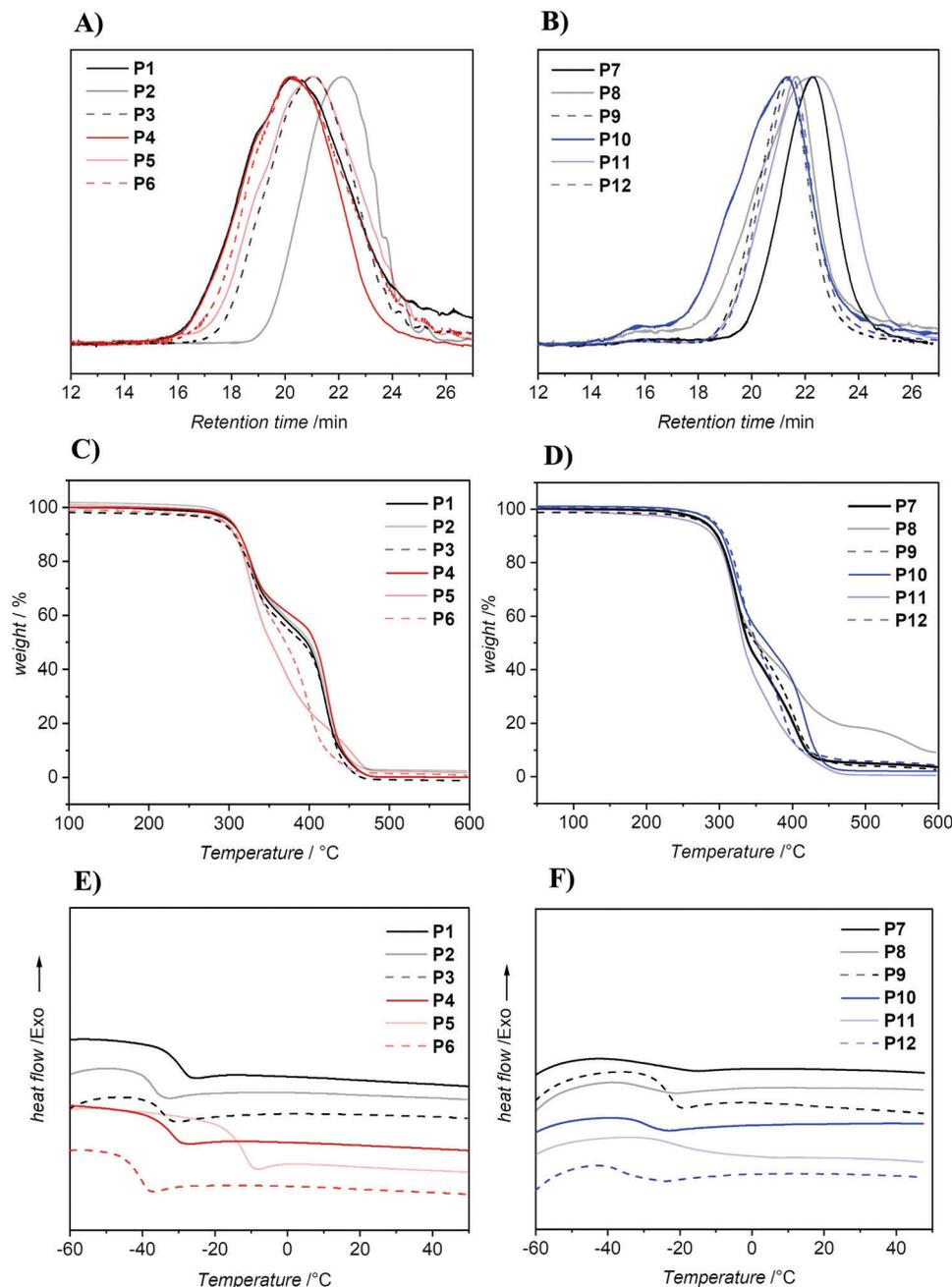
**ADVANCED
SCIENCE NEWS**

www.advancedsciencenews.com

M acro-
olecular
Chemistry and Physics
www.mcp-journal.de

Figure 2. Comparative: A) SEC traces of polymer **P1-P6** obtained from the reaction of **M1** and dithiol derivatives; B) SEC traces of polymer **P7–P12** synthesized from **M2** and dithiol derivatives; C) TGA of **P1-P6** derived from **M1** with various dithiols; (D) TGA of **P7–P12** derived from **M2** in the presence of diverse dithiols; E) DSC curves of **P1-P6**; and (F) DSC curves of **P7-P12**, respectively.

2.4. Thermal Properties of 1,5-DS-T Decorated Polymers

Thermogravimetric analysis (TGA) was applied in order to detect the thermal properties of the novel developed polymers; particularly, we have determined the composition temperature ($T_{d, 5\%}$), which is defined as the temperature at 5% weight loss. As shown in Figure 2C,D and Table 1, a multistep degradation pattern was observed with a $T_{d, 5\%}$ of approximately ≈300 °C and ~280°C under inert conditions (i.e., nitrogen gas) for **P1–P6** (Figure 2C) and **P7–P12** (Figure 2D), respectively, resulting from the poly-

merizations of **M1** and **M2** with a series of the dithiols shown in Scheme 2B. The first degradation step occurred approximately between 280 and 395 °C followed by the second step ≈400 to 470 °C. The first degradation can be attributed to the elimination of tetrazole pendant group, while the second step is relevant to the backbone degradation. Importantly, no char residue was observed for most of the polymers, aside for polymer **P8**. In addition, the different chain length of the dithiol derivatives had relatively small influence on $T_{d,5\%}$ as can be seen in Figure 2C,D (shorter length of **P1** or **P7**, versus longer length of **P4** or **P10**).
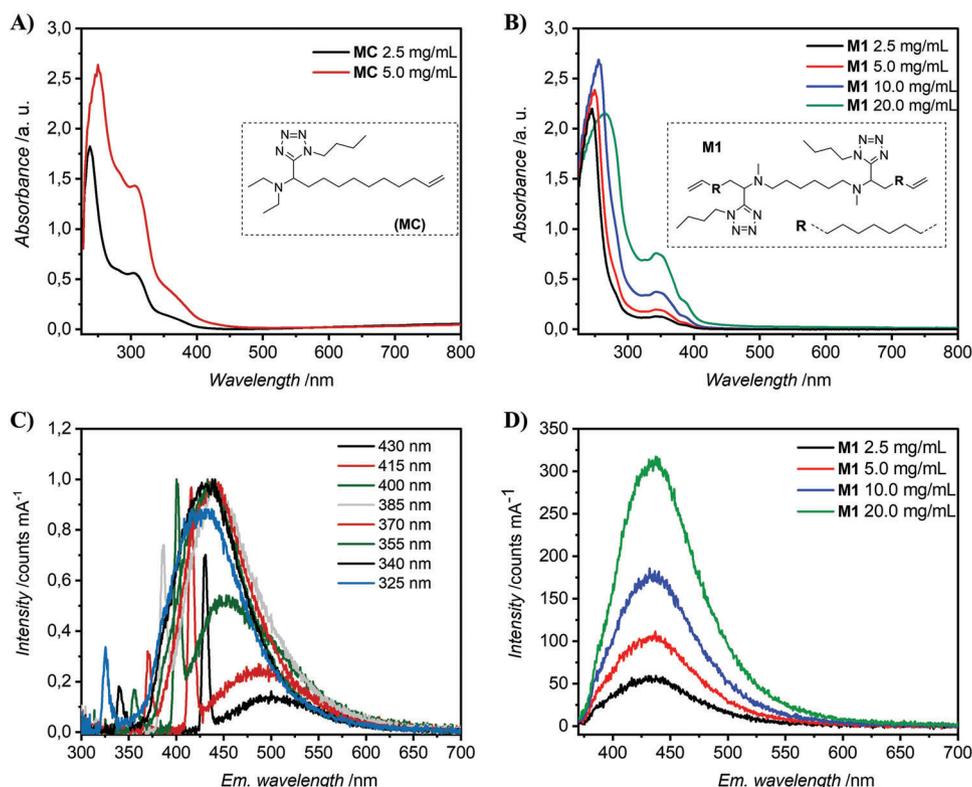
ADVANCED
SCIENCE NEWS

www.advancedsciencenews.com

Macro-
molecular
Chemistry and Physics

www.mcp-journal.de

Figure 3. A,B): Absorption traces of **MC** and **M1**, respectively, at different concentrations in MeOH (for **MC**: black: 2.5 mg mL^{-1}, red: 5.0 mg mL^{-1}; for **M1**: black: 2.5 mg mL^{-1}, red: 5.0 mg mL^{-1}, blue: 10.0 mg mL^{-1}, green: 20.0 mg mL^{-1}). C) Emission spectra of **M1** at various excitation wavelengths (from 325 to 430 nm) in MeOH (c = 20 mg mL^{-1}). D) Emission spectra of **M1** at different concentrations (black: 2.5 mg mL^{-1}, red: 5.0 mg mL^{-1}, blue: 10.0 mg mL^{-1}, green: 20.0 mg mL^{-1}) in MeOH (298 K) at λ_{ex} = 355 nm.

Whereas TGA curves of **P5** and **P11**, which contain hydrogen-bond interaction originating from **DT5**, apparently, have shown a dramatic decrease in the composition temperature ($T_{d, 5\%}$).

Next, the thermal transitions of the polymers were investigated via differential scanning calorimetry (DSC), (Figure 2E,F). In general, the DSC studies indicated that the polymers were in an amorphous state, being characterized by low glass-transition temperature (T_g) values ($T_g < -10$ °C). Moreover, it was detected that **P1–P6** (polymers derived from **M1**) featured a lower glass transition temperature than **P7–P12** (polymers derived from **M2**). Indeed, we have postulated that by reducing the distance between the rigid units (particularly in the 1,5-tetrazole-decorated units), we could deliver polymers with higher T_g values. In regard of the impact of dithiol derivatives, **DT6** further increased the distance and the chain-flexibility between the rigid backbone components, thus leading to the lowest observed T_g of the dithiol linkers at −42 °C for **P6** and −32 °C for **P12**, respectively.

2.5. Optical Properties of 1,5-DS-T Decorated Organic Molecules and Polymers

Conventional luminescent polymers usually are integrated with extended $\pi-\pi$ conjugated structures that suffer from associated aggregation-caused quenching and complex synthesis. Therefore, there is a huge demand for stand-alone luminescent polymers that can circumvent these drawbacks and can be em-

ployed in diverse applications. Indeed, the synthesized compounds (e.g., small molecules in addition to the polymers) have the potential to present luminescent properties,[45] since electron-rich heteroatoms (i.e., N, O, and P),[46,47] hydroxyl (OH), amino (NH$_2$), carbonyl (C=O), cyano (CN),[30] carboxyl (COOH),[36] amide (CONH),[48] anhydride[49] and carbon–carbon double bonds (C=C)[50] can form diverse clusters upon aggregation, that is termed as the clustering-triggered emission (CTE). Therefore, we have investigated the respective photophysical properties via UV–vis and Fluorescence spectroscopy. Due to simplicity, we performed preliminary investigations by analyzing the absorption spectra of **MC** and **M1** (which are chemically similar to **M2**) in MeOH. On the one hand, the UV-vis spectrum of **MC** depicted the following absorbances and weak fluorescence at ≈238, 304, and ≈364 nm, which in turn shifted to higher wavelengths (250, 308, and ≈374 nm, respectively) with the increment of concentration (from 2.5 mg mL^{-1} to 5.0 mg mL^{-1} in MeOH) as shown in **Figure 3**A.

Furthermore, as the concentration increased, an increment in the absorption intensity was also observed (Figure 3A). The calculated quantum yield (QY) of **MC** was Φ_{MC} = 1.92%, (Figure S13, Supporting Information) which can be related with low luminescence materials. On the other hand, monomer **M1** showed slightly different behavior (Figure 3A), i.e., the absorption spectrum (at concentration of 2.5 mg mL^{-1} in MeOH) featured two maxima centered at 247 and 346 nm in addition to an absorption band at 389 nm as a shoulder. The absorption band, which was
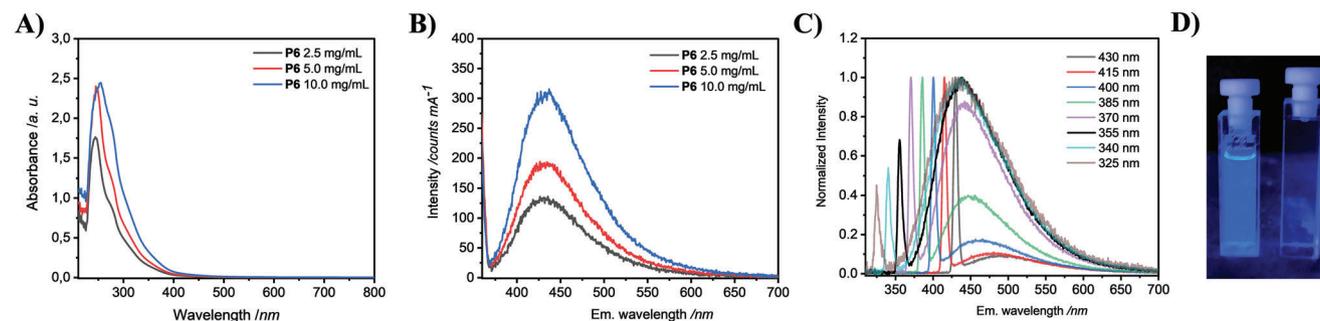
**ADVANCED
SCIENCE NEWS**

www.advancedsciencenews.com

|M acro-
molecular

Chemistry and Physics

www.mcp-journal.de

Figure 4. A,B): Absorption and emission (λ_{ex} = 355 nm) traces of **P6**, respectively, at different concentrations in DCM (black: 2.5 mg mL^{-1}, red: 5.0 mg mL^{-1}; blue: 10.0 mg mL^{-1}). C) Emission spectra of **P6** at various excitation wavelengths (from 325 to 430 nm) in DCM (c = 10.0 mg mL^{-1}). D) Photographs were taken under 365 nm UV light of **P6** (10.0 mg mL^{-1} in DCM, left) and pure DCM (right).

detected at 247 nm, was shifted to higher wavelength at 270 nm with the increased concentration from 2.5 to 20.0 mg mL^{-1}, while the absorption intensity at first has increased and decreased at concentration of 20.0 mg mL^{-1} (Figure 3B). On the contrary, the absorption bands at 346 and 389 nm have remained practically in the same wavelength range accompanied with an increment in the absorption intensity (Figure 3B). To get more information about the photophysical properties of **M1**, we have further determined its emissions by varying excitation wavelengths (λ_{ex}). In fact, the fluorescence emission of **M1** (in Figure 3C) showed a significant change upon different λ_{ex} values from 325 to 420 nm, i.e., the photoluminescence peak shifts to longer wavelengths and its intensity decreases rapidly, with the strongest peak excited at the absorption band. This is a compelling photoluminescence phenomenon that is generally exhibited by nonconventional luminescent materials (either small molecules or polymers). The latter behavior is mainly attributed to the materials containing different chromophores with degenerate energy levels. Furthermore, as concentration is a crucial parameter to adjust nonconventional intrinsic luminescence behavior of small molecules and polymers, and to identify emission centers,[51] fluorescence emission spectra of **M1** solutions with different concentrations were measured at λ_{ex} = 355 nm (Figure 3D). In fact, a significant increase of fluorescence emission intensity was observed in addition to a slight redshift of the emission band located at 427 nm to a higher wavelength of 440 nm, when the **M1** concentration was varied from 2.5 to 20.0 mg mL^{-1}. Thus, we inferred that **M1** possessed the cluster-induced emission characteristic. In fact, it has been reported[49,52] that nonconventional fluorescence is usually observed for materials in the aggregated state or solid phase, and was associated with the interaction of carbonyl groups, $n-\pi^*$ interactions occurring due to the overlap of the n orbitals of lone pair electrons of N, O, or S atoms and the adjacent antibonding π^* orbitals of carbonyl groups, or other double bonds, and $\pi-\pi^*$ interactions of double and/or triple bonds. Subsequently, we examined the exemplary **M1**-derived polymers **P1**, **P4**, and **P6** and compared them to **M2**-derived polymers **P7**, **P10**, and **P12** regarding their optical properties. In fact, the UV-vis spectra of all polymers depicted a similar behavior, which was comparative to monomer **M1**. In other words, an absorbance max at ≈245 nm with a shoulder peak at 343 nm was observed for all polymers. The increase of the concentration (from 2.5 to 10.0 mg mL^{-1} in DCM) was accompanied with an increment of the absorption in-

tensity and in a redshift of the absorbance maxima (to ≈254 nm) in addition to an extension of the tail extended to the visible region, as it is shown in **Figure 4**A; along, Figures S14 and S15 in the Supporting Information. Negligible impact on the intensity of the absorption was observed by varying the type of the dithiols (**DT1** (1,4-butanedithiol), **DT4** (1,9-nonanedithiol) and **DT6** (3,6-dioxa-1,8-octanedithiol) polymerized with monomer **M2** (see Figure S15, Supporting Information). Polymers (**P1**, **P4**, and **P6**) derived from **M1** showed clear dependency on the dithiol used, i.e., the incorporation of **DT6** in polymer **P6** resulted in the maximum absorption intensity (compare Figure 4A and Figure S14, Supporting Information). Furthermore, with increasing concentration, visible blue emission was observed for all polymers when it gets to 10.0 mg mL^{-1}. As it is depicted in Figures 4B in addition to Figures S14 and S15, Supporting Information, the photoluminescence intensity progressively has become higher and redshifted as the concentration increased from 2.5 to 10.0 mg mL^{-1} with an E_m (photoluminescent emission) at 438 nm (λ_{ex} = 355 nm), which can be ascribed to the clustering of tetrazole and thioether moieties along with the conformation rigidification.

Moreover, the emission spectra of the solution of **P6** (10.0 mg mL^{-1}) with varying λ_{ex} values also verified the presence of different emission centers (Figure 4C). Actually, the E_m values were conspicuously redshifted as λ_{ex} has increased from 325 to 430 nm. Furthermore, when dissolved in different solvents, such as MeOH, the emission spectra of all polymers exhibit a slightly varied emission profile (Figure S16, Supporting Information), indicating the different emissive clusters in varying solvents. The photographs of all polymers in DCM under the illumination of a 365 nm UV lamp are shown in Figure 4D in addition to Figures S14 and S15, Supporting Information. Taking **P6** for example, multiple intra- and intermolecular interactions like arising from $n-\pi^*$ or $\pi-\pi^*$ transitions between electron-rich –C=C-, –N=N– and –N–N–, and the conjugated aromatic tetrazole units can be considered as the possible mainspring for cluster triggered emission. Such effective through space electronic communication in addition to the rigidified conformations could be postulated as a reason for the emission of the clusters upon UV excitation. Nevertheless, density functional theory calculations are essential in order further understand the fluorescence behavior of those classes of polymers and the respective small molecules at the molecular level.

3. Conclusion

To conclude, we have demonstrated the first attempt for the synthesis of the tetrazole-decorated monomers via Ugi-azide four-multicomponent reaction (UA-4MCR) and their respective polymerization via thiol-ene chemistry. The synthetic concept was primarily established with a bis-1,5-disubstituted-1*H*-tetrazole (**bis-1,5-DS-T**) decorated model compound, which was subsequently examined via a model thiol-ene reaction to ensure that the thiol derivatives do not undergo any side reactions with the respective tetrazole units under a light-induced thiol-ene addition reaction. Accordingly, the synthesis of two α,ω-diene monomers decorated with **bis-1,5-DS-T** units was successfully conducted. Monomers were fully characterized, and the respective light-induced thiol-ene polyaddition reaction with different dithiol derivatives allowed for the construction of diverse polymers decorated with **bis-1,5-DS-T**. Importantly, detailed NMR, SEC, ATR-IR characterization confirmed the successful polymerization and showed that the **1,5-DS-T** moiety remained intact during the polymerization process. Furthermore, the thermal and optical properties of the polymers have been investigated, revealing that the tetrazole-decorated polymers show two-step degradation process with stability up to 300 °C. Critically, one of the objectives of this research was to reveal the cluster-triggering properties of **1,5-DS-T** containing polymers, potentially paving the way toward nonconventional luminescent polymeric materials. Indeed, further studies on the synthesis of main-chain **1,5-DS-T** containing polymers and their post-polymerization modification along the in-depth understanding of the unconventional luminescent properties are currently underway. Last but not least, the potential applications in the field of biomedicine because of the unique properties (e.g., antibacterial, anticancer) are also under investigation.

Supporting Information

Supporting Information is available from the Wiley Online Library or from the author.

Acknowledgements

Conflict of Interest

The authors declare no conflict of interest.

Data Availability Statement

The data that support the findings of this study are available from the corresponding author upon reasonable request.

Keywords

[1] N. Kerru, L. Gummidi, S. Maddila, K. K. Gangu, S. B. Jonnalagadda, *Molecules* **2020**, *25*, 1909.

[2] M. Baumann, I. R. Baxendale, S. V. Ley, N. Nikbin, *Beilstein J. Org. Chem.* **2011**, *7*, 442.

[3] C. G. Neochoritis, T. Zhao, A. Dömling, *Chem. Rev.* **2019**, *119*, 1970.

[4] J. A. Bladin, *Ber. Dtsch. Chem. Ges.* **1885**, *18*, 1544.

[5] A. Al-Mulla, *Der Pharma Chem.* **2017**, *9*, 141.

[6] V. A. Ostrovskii, E. A. Popova, R. E. Trifonov, *Adv. Heterocycl. Chem.* **2017**, *123*, 1.

[7] T. Zhao, K. Kurpiewska, J. Kalinowska-Tłuslcik, E. Herdtweck, A. Dömling, *Chem. - Eur. J.* **2016**, *22*, 3009.

[8] A. Maleki, A. Sarvary, *RSC Adv.* **2015**, *5*, 60938.

[9] E. Bakangura, Y. He, X. Ge, Y. Zhu, L. Wu, J. Ran, C. Cheng, K. Emmanuel, Z. Yang, T. Xu, *Chem. Sci. Eng.* **2018**, *12*, 306.

[10] S. M. Sproll, *Investigation of Nitrogen-Rich Polymers Based on Tetrazoles and Triazoles*, Dissertation Ludwig-Maximilians-Universität, München **2009**.

[11] M. Mahkam, M. Nabati, A. Latifpour, J. Aboudi, *Des. Monomers Polym.* **2014**, *17*, 453.

[12] W. R. Carpenter, US Pat. 3,386,968, **1968**.

[13] E. Zakerzadeh, R. Salehi, M. Mahkam, *Drug Dev. Ind. Pharm.* **2017**, *43*, 1963.

[14] N. V. Tsarevsky, K. V. Bernaerts, B. Dufour, F. E. Du Prez, K. Matyjaszewski, *Macromolecules* **2004**, *37*, 9308.

[15] J. Aronson, *The Synthesis and Characterization of Energetic Materials from Sodium Azide*, Georgia Institute of Technology, Atalanta (GE) **2004**.

[16] a) C. G. Miller, G. K. Williams, Automotive Systems Laboratory Inc, assignee. *US Pat. 7776169B2*, **2010**. b) M.-R. Huang, X.-G. Li, S.-X. Li, W. Zhang, *React. Funct. Polym.* **2004**, *59*, 53.

[17] F. M. Betzler, R. Boller, A. Grossmann, T. M. Klapötke, *Z. Naturforsch. B* **2013**, *68*, 714.

[18] T. M. Klapötke, S. M. Sproll, *J. Polym. Sci., Part A* **2010**, *48*, 122.

[19] W. G. Finnegan, R. A. Henry, S. Skolnik, *U. S. Patents 3004959*, **1961**.

[20] C. G. Miller, G. K. Williams, *U. S. Patents. 264982*, **2007**.

[21] P. N. Gaponik, O. A. Ivashkevich, V. P. Karavai, A. I. Lesnikovich, N. I. Chernavina, G. T. Sukhanov, G. A. Gareev, *Angew. Makromol. Chem.* **1994**, *219*, 77.

[22] F. M. Betzler, T. M. Klapötke, S. M. Sproll, *Eur. J. Org. Chem.* **2013**, *2013*, 509.

[23] E. Marqués-López, R. P. Herrera, *Multicomponent Reactions: Concepts and Applications for Design and Synthesis*, John Wiley & Sons, Hoboken, New Jersey **2015**.

[24] E. Marqués-López, R. P. Herrera, In: *Multicomponent Reactions: Concepts and Applications for Design and Synthesis* (Eds: R. P. Herrera, E. Marqués-López), John Wiley & Sons, Hoboken, NJ, USA, **2015**.

[25] M. A. Fouad, H. Abdel-Hamid, M. S. Ayoup, *RSC Adv.* **2020**, *10*, 42644.

[26] I. Ugi, R. Meyr, C. Steinbruckner, *Angew. Chem.* **1959**, *71*, 373.

[27] I. Ugi, C. Steinbrückner, *Chem. Ber.* **1961**, *94*, 734.

[28] I. V. Kutovaya, D. P. Zarezin, O. I. Shmatova, V. G. Nenajdenko, *Eur. J. Org. Chem.* **2019**, *2019*, 3908.

[29] H. Leonards, S. Engelhardt, A. Hoffmann, L. Pongratz, S. Schriever, J. Bläsius, M. M. Wehner, A. Gillner, Proc. SPIE 9353, San Francisco, California, USA, **2015**.

[30] N. K. Singha, H. Schlaad, *Functional Polymers by Post-Polymerization Modification: Concepts, Guidelines, and Applications* (Eds: P. Theato, H.-A. Klok), Wiley-VCH Verlag GmbH & Co. KGaA, Weinheim **2013**.

**ADVANCED
SCIENCE NEWS**

www.advancedsciencenews.com

**Macro-
molecular
Chemistry and Physics**

www.mcp-journal.de

[31] W. Feng, L. Li, C. Yang, A. Welle, O. Trapp, P. A. Levkin, *Angew. Chem.* **2015**, *127*, 8856.

[32] L. Santhosh, S. R. Nagamangala, V. M. Thimmalapura, S. V. Vommina, *ChemistrySelect* **2017**, *2*, 5497.

[33] Whereas there are various aldehyde derivatives, bio-based alkenes (i.e., pentenal and 10-undecenal, which are derived by pyrolysis and reduction from pentanoic acid and castor oil, respectively) were selected as a renewable natural resource.

[34] *N, N*-Dimethyl-1,6-hexanediamine was chosen to mimic adipic acid, which is a precursor for nylon synthesis as a bio-based derivative.

[35] T. Saegusa, S. Kobayashi, Y. Ito, *J. Org. Chem.* **1970**, *35*, 2118.

[36] K. Singh, S. Sharma, *Tetrahedron Lett.* **2017**, *58*, 197.

[37] A. L. Barthelon, L. El Kaïm, M. Gizolme, L. Grimaud, *Eur. J. Org. Chem.* **2008**, *2008*, 5974.

[38] Density values for dithiols: **DT1**: 1.04 g/mL, **DT2**: 0.98 g/mL, **DT3**: 0.97 g/mL; **DT5**: crystalline; **DT6**: 1.12 g/mL.

[39] H. R. Kricheldorf, *Macromol. Rapid Commun.* **2008**, *29*, 1695.

[40] a) T. Endo, T. Higashihara, *ACS Omega* **2022**, *7*, 8753; b) C. Wallis, M. Bonhomme, J. F. Fabre, Z. Mouloungui, *e-Polymers* **2018**, *18*, 229.

[41] H. R. Kricheldorf, G. Schwarz, *Macromol. Rapid Commun.* **2003**, *24*, 359.

[42] S. M. Weidner, H. R. Kricheldorf, F. Scheliga, *J. Polym. Sci., Part A: Polym. Chem.* **2016**, *54*, 197.

[43] O. Okay, S. K. Reddy, C. N. Bowman, *Macromolecules* **2005**, *38*, 4501.

[44] H. R. Kricheldorf, S. M. Weidner, F. Scheliga, *Macromol. Symp.* **2017**, *375*, 1600169.

[45] a) H. Jacobson, C. O. Beckmann, W. H. Stockmayer, *J. Chem. Phys.* **1950**, *18*, 1607; b) H. Jacobson, W. H. Stockmayer, *J. Chem. Phys.* **1950**, *18*, 1600; c) a general review on the topic: P. Knops, N. Sendhoff, H.-B. Mekelburger, F. Vögtle, *Top Curr. Chem.* **1991**, *161*, 1.

[46] C. N. S. S. P. Kumar, D. K. Parida, A. Santhoshi, A. K. Kota, B. Sridhar, V. J. Rao, *MedChemComm* **2011**, *2*, 486.

[47] R.-B. Wang, W.-Z. Yuan, X.-Y. Zhu, *Chin. J. Polym. Sci.* **2015**, *33*, 680.

[48] J. Yan, B. Zheng, D. Pan, R. Yang, Y. Xu, L. Wang, M. Yang, *Polym. Chem.* **2015**, *6*, 6133.

[49] R. B. Restani, P.-C. I. Morgado, M. P. Ribeiro, I.-D. J. Correia, A. Aguiar-Ricardo, V. D. B., *Bonifácio Angew. Chem., Int. Ed.* **2012**, *51*, 5162.

[50] X. Zhou, W. Luo, H. Nie, L. Xu, R. Hu, Z. Zhao, A. Qin, B. Z. Tang, *J Mater Chem* **2017**, *5*, 4775.

[51] L. Yang, L. Wang, C. Cui, J. Lei, J. Zhang, *Chem. Commun.* **2016**, *52*, 6154.

[52] C. Shang, Y. Zhao, J. Long, Y. Ji, H. Wang, *J. Mater. Chem. C* **2020**, *8*, 1017.

[53] a) C. Shang, N. Wei, H. Zhuo, Y. Shao, Q. Zhang, Z. Zhang, H. Wang, *J Mater Chem* **2017**, *5*, 8082; b) Y. Du, H. Yan, W. Huang, F.u Chai, S. Niu, *ACS Sustainable Chem. Eng.* **2017**, *5*, 6139.